Journal of Materials Chemistry C

Accepted Manuscript

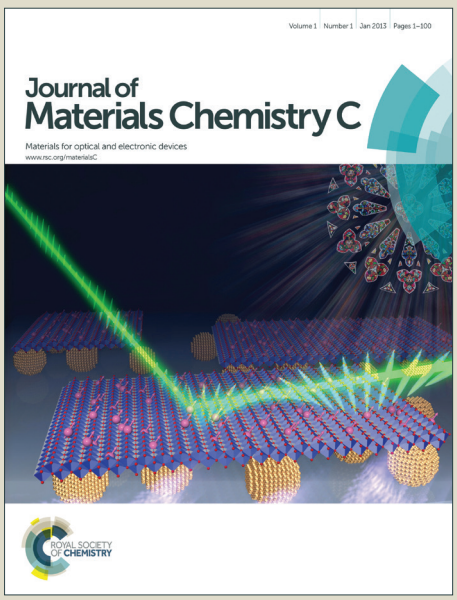

ROYAL SOCIETY OF CHEMISTRY

www.rsc.org/materialsC

Journal of
Materials Chemistry C

RSCPublishing

PAPER

Aggregation-induced and crystallization-enhanced emissions with time-dependent of a new Schiff-base family based on benzimidazole

Yuanle Cao[a], Mingdi Yang[a, b, *], Yang Wang[a], HongPing Zhou[a, *], Jun Zheng[c], Xiuzhen Zhang[a], Jieying Wu[a], Yupeng Tian[a] and Zongquan Wu[d]

A new Schiff-base family containing [4-(1H-benzimidazole-2-yl)-phenyl]-bis-(4-ethoxy-phenyl)-amine has been synthesized feasibly through condensation reaction. All the derivatives possessing aggregation-induced and crystallization-enhanced emission (AIE and CEE) properties, which show time-dependent characteristic at a concentration of 10 μM, are studied in detail by scanning electron microscope (SEM) and transmission electron microscope (TEM). Different aggregation forms and the growth of crystal of the compounds, could be responsible for the notably different degrees of the fluorescence enhancement.

www.rsc.org/materialsC

Introduction

Organic fluorescent materials have been attracted intensive interest because of their potential applications in organic light-emitting diodes (OLED), fluorescent sensors, etc.[1] However, many dyes emit strongly when dissolved in their good solvents but become weak luminescence when fabricated into solid films or aggregated in their poor solvents.[2] This phenomenon is notoriously known as aggregation-caused quenching (ACQ).

The ACQ effect has greatly limit the applications of organic luminescent materials and has driven researchers to seek anti-ACQ materials with higher efficiency in the aggregated state than in the dissolved state. Several anti-ACQ materials were reported by Tang *et al*. and Park *et al*.[4] in 2001 and 2002, respectively, and these substances are termed aggregation-induced emission (AIE) and aggregation-induced enhancement emission (AIEE) materials. Herein, some materials among them show special phenomenon of AIE or AIEE in the aqueous mixtures as the form of crystal state, which was designated as crystallization-enhanced emission (CEE).[5] Many crystalline AIE materials have been found to exhibit high fluorescence efficiencies compared to their amorphous counterparts. The AIE or CEE effect was previously attributed to the restricted intramolecular rotation (RIR) mechanism. Although the mechanism of AIE or CEE have been studied for a period of time, the number of the AIE or CEE materials are quite limited, for example, silole-based compounds and arylethene derivatives.[6] To further enlarge the family of the specific AIE-active compounds, it is necessary to carry out more extensive investigations in this field.

Recently, the synthesis and application of triphenylamine (TPA) derivatives as emissive materials have been of great interest for chemists and material scientists due to their charge-transport properties, and thermal stability.[7] TPA derivatives, however, usually give a strong emission in organic solvent but suffer from the notorious effect of ACQ in the condensed phase. Benzimidazole, a conjugated compound with good bioactivity, is usually used in medical intermediate.[8] Combination of two compounds may lead to the generation of a new system with enhanced conjugation and bioactivity. Small aromatic ring attached to benzimidazole with single bond may activate the radiative transition channel in some extent, which could endow the compounds possess AIE or AIEE properties.

We are interested in and have worked on exploration of new AIE or CEE systems.[9] In this work, we synthesis six novel TPA-substituted benzimidazole-based conjugated Schiff bases. During the study, we discovered that the compounds emit fluorescence in the solvent mixtures with low water contents containing crystal but become non-luminescent even in the mixtures with high water contents containing homogeneous nano-particles, which can be attributed to the AIE and CEE process. Intramolecular motions of the compounds remain active in the amorphous phase and can be suppressed by crystal formation, thus causing the novel CEE effect. All the AIE and CEE phenomena of the compounds are accompanied by the intensity enhancement of time-dependent. This behavior may be induced by the constantly changing size and morphology of nanoparticles under the impact of solvent such as water.[10]

Results and Discussion

Synthesis

Synthetic routes of compounds **1-6** and their intermediates were depicted in **Scheme 1**. The detailed procedures for the syntheses of the intermediates and final products are described in the experimental section. The targeted compounds **1-6** were obtained by the condensation of aldehyde and amine.

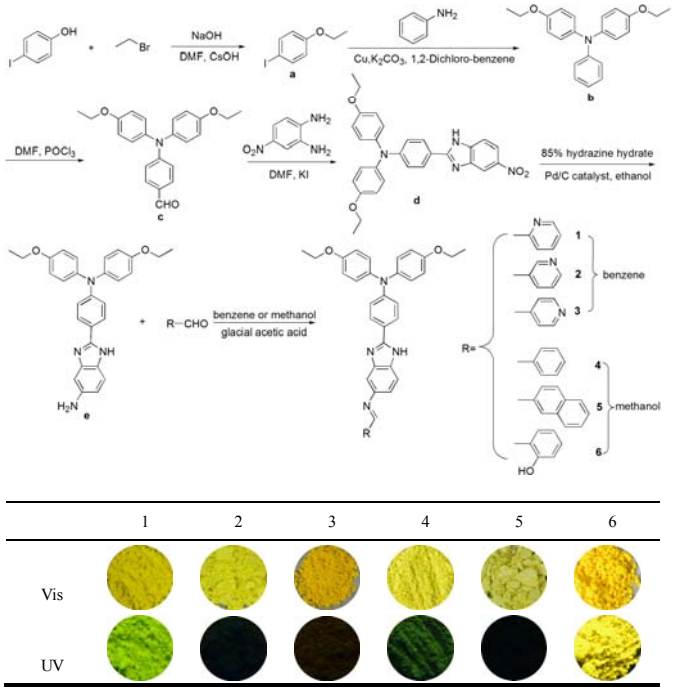

Scheme 1 Synthetic routes of compounds **1-6** and their solid photographs taken under visible and UV light.

Absorption and Photoluminescence Properties

Figures 1 and 2 show the absorption and fluorescence spectra of compounds **1** and **5** (the others in **Fig. S1** and **Fig. S2**) in different polar solvents (dichloromethane (DCM), tetrahydrofuran (THF), ethanol, acetonitrile, N,N-dimethyl formamide (DMF) and dimethylsulfoxide (DMSO)).

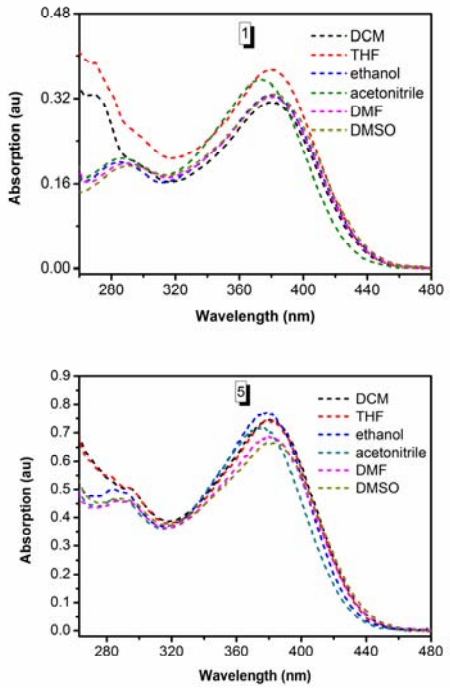

Fig. 1 Absorption spectra of compounds **1** and **5** in different polar solvents. Concentration of the solutions: 10 μM.

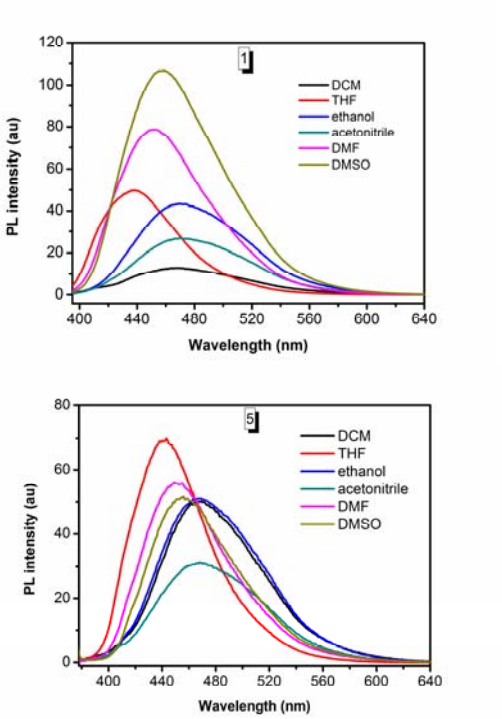

Fig. 2 Fluorescence spectra of compounds **1** and **5** in different polar solvents (10 μM).

As seen in **Fig. 1** and **Table S1**, The polarity of solvents had little effect on the absorption wavelengths of compounds **1** and **5** (**2-4**, **6** in **Fig. S1**) but exerted a great effect on the photoluminescence (PL) emission (**1** and **5** in **Fig. 2**, **2-4**, **6** in **Fig. S2**). For example, the maximum absorption wavelength (λ_a) of compound **1** located at 373-381 nm, however, the maximum emission wavelength (λ_e) varied from 437 nm to 470 nm. The λ_a and λ_e (**Table S1**) of **1-3** in different solvents are almost the same, which reveals that different location of N in pyridine has no obvious effect on the maximum emission wavelengths of **1-3**.

To better understand the photophysical properties of the compounds, we performed theoretical calculations with the density functional of B3LYP/6-31G(d). The optimized geometries and HOMO (Highest Occupied Molecular Orbital)/LUMO (Lowest Unoccupied Molecular Orbital) plots of **1-6** are illustrated in **Fig. 3**. All the molecules adopt twisted non-planar conformations at the terminal aromatic ring, which are favorable for active intramolecular rotations of aromatic ring in pure solutions. In spite of the values of band gap (ΔE_g) are different (**Table S2**), they have very similar maximum absorption and emission wavelengths in the same solvents, indicating the potential influence of molecular rotation on band gaps in the excited state.

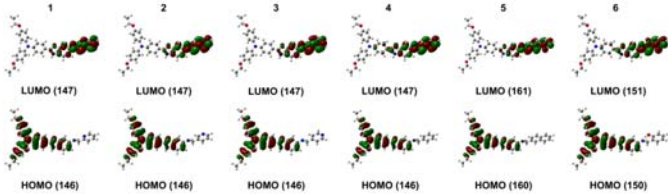

Fig. 3 Energy level and electron density distribution of frontier orbitals of compounds **1-6**.

Obviously, the electron clouds of HOMO and LUMO of compounds **1-6** are dominated by the triphenylamine section and aromatic ring at the end of the molecules, respectively, which means that their absorption and emission stem from the ICT

(Intramolecular Charge Transfer) transitions primarily. However, emission behavior of compounds **1-6** in solvents as described above is strikingly different from that of conventional ICT systems, which are nonfluorescent in highly polar solvents but intensely emissive in nonpolar solvents. Thus the formation of aggregation may restrain the ICT process in the mixture solution to some extent, which is helpful for the light emission.[11]

AIE and CEE Phenomena

The dilute THF solutions of **1-6** (1×10^{-5} mol/L) were transparent and gave very faint lights with emission maximums peak in the neighborhood of 450 nm when excited at 380 nm at room temperature (**Table 1**).

Table 1 Fluorescence quantum yield (QY) obtained after water was injected for 24 hours.

QY	f_w= 0 %	f_w= 30 %	f_w= 60 %	f_w= 90 %
1	<0.1 %	37.2 %	17.8 %	5.4 %
2	<0.1 %	26.6 %	11.3 %	1.8 %
3	<0.1 %	27.7 %	7.9 %	1.9 %
4	<0.1 %	28.0 %	12.1 %	<0.1 %
5	<0.1 %	25.4 %	12.2 %	1.9 %
6	<0.1 %	35.3 %	14.3 %	0.3 %

f_w: water fraction.

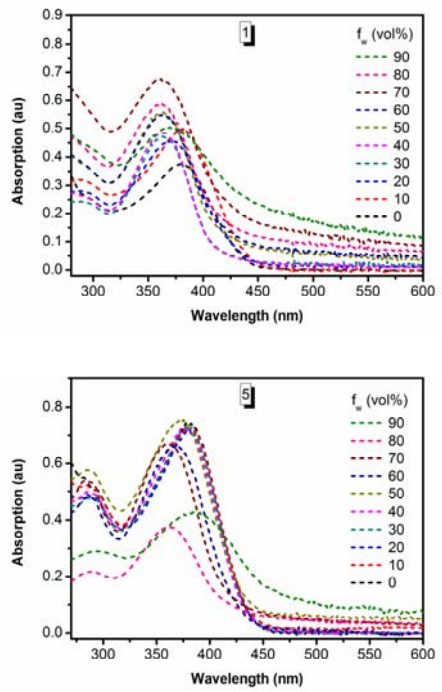

Fig. 4 UV absorption spectra of **1** and **5** in water/THF mixtures with different volume fractions of water after water was injected for 1 h (10 μM).

The absorption spectra of **1** and **5** in the THF/water mixtures are shown in **Fig. 4**. The spectrum profile was virtually unchanged when water of low fraction was injected into the THF solution. However, the absorption curves of **1-6** in the THF/water mixtures with relatively high water fraction (≥ 60%) hardly decay to zero even in the long wavelength region, indicative of existence of aggregative species in these solvent mixtures.[12] The maximum absorption wavelength of **1** undergoes a blue-shift from 381 nm (in pure THF solvent) to 361 nm (at 50% water fraction), and then red-shift to 373 nm (at 90% water contents), indicating that the during of emitting species self-assemble, the states of aggregation may changed. The same tendency can also be found in the absorption spectra of other compounds (**Fig. S3**).

Behaviors of luminescence in water/THF mixtures with different water contents after water was injected for 24 hours are shown in **Fig. 5** (**2-4**, **6** in **Fig. S4**). In pure THF, the emission of the compounds **are** very weak and virtually invisible. However, strong blue and cyan emission can be exhibited in solvent mixtures with 30% and 60% water contents, respectively. The absorption and emission behaviors of **1** in the pure THF and THF/water mixtures may be understood as follows. In the isolated state, namely, molecule completely dissolved in good solvent, the active intramolecular rotations of terminal aromatic ring have effectively deactivated its excited species, hence the faint light emission can be observed. Since the formation of aggregation can rigidify the molecular conformation and thus block the nonraditive relaxation channel, the excited state decays radiatively. As a result, **1** becomes highly emission in the aggregation state. As the proportion of water further increase to a certain degree (90%), no fluorescence can be observed again (insets in **Fig. 5** and **Fig. S4**). All compounds show a emission enhancement at low water fraction but a decrease at high water fraction, which exhibits a down-top-down "Λ" pattern. This phenomenon was often observed in some compounds with AIE properties, but the reasons remain unclear.[13] To better understand the luminescence behavior and mechanism of the compounds in solvent mixtures, we carried out the following study in detail.

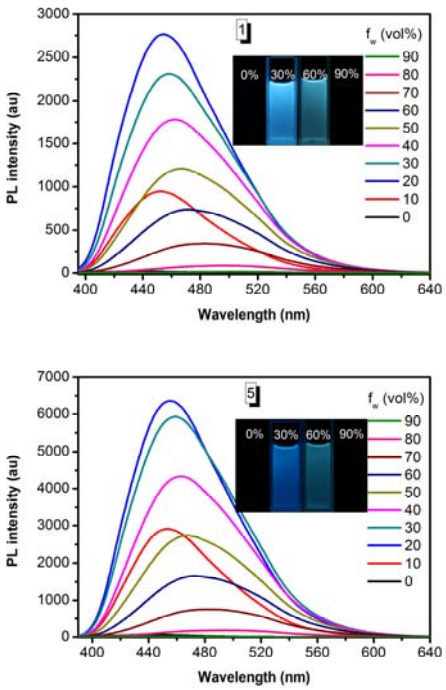

Fig. 5 PL spectra of the dilute solutions of **1** and **5** in water/THF mixtures with different volume fractions of water (excitation wavelength = 365 nm) after water was injected for 24 hours (10 μM). The insets show the emission images of **1** and **5** in pure THF as well as solvent mixtures with 30%, 60% and 90% water contents taken under 365 nm UV illumination at room temperature (10 μM), respectively.

As can be seen in **Table 1**, the fluorescence quantum yield (Φ_F) of compounds **1-6** in the water fraction of 30% are higher than that in the water fractions of 60% and 90%. Hence, the addition of water may effectively influence the conformation of molecules in some extent. The similar quenched emission and low fluorescence efficiency (**Table 1**) of **1-6** in pure THF and mixtures with high

water contents (>80%) suggest that they may possess properties of AIEE.[14]

To further prove our hypothesis, we followed the time course of spectral evolution of **1-6** (**1**, **5** in **Fig. 6**, **2-4** and **6** in **Fig. S5**) in mixtures with different water contents. Amusingly, the emission intensity of a prepared aqueous mixture change constantly with time at room temperature. As depicted in **Fig. 6**, the PL spectra of compounds **1** and **5** show a remarkable enhancement in the emission intensity in low water fractions. In contrast, almost no changes in the PL spectra of the compounds are observed in the aqueous mixtures over 80% water contents, even after the mixture has been allowed to stand for as long as 24 h. As the compounds have a good solubleness in a low hydrous mixture, there is hardly any nanoparticles available within a short time. However, as time passed, molecules may gradually self-assemble to crystal particles, giving a fluorescence enhancement of time-dependent.[15] On the other hand, in the solvent mixture with 90% water content, the molecules may disperse to amorphous nanoparticles. From the absorption with no trailed peak of compounds **1-6** in low water fraction in **Fig. 4** and the obvious enhancement of emission in the mixture of low water faction (<30%), one can find that despite there is no tailed peak in mixture with low water contents, the emission can still enhance in a lasting time. The fluorescent intensity enhancement of **1-6** with 30% water fractions increased from 32, 17, 14, 2, 32, 0.4 times to 102, 35, 62, 10, 90, 9 times after water was added for 24 hours. **Fig. 7** shows the photographs of solution mixture taken under the UV illumination with 50% water contents. As time goes from 0 min, 30 min to 50 min, the fluorescence intensity shows a enhancement of 30 times and 45 times compared with that of 0 min, respectively.

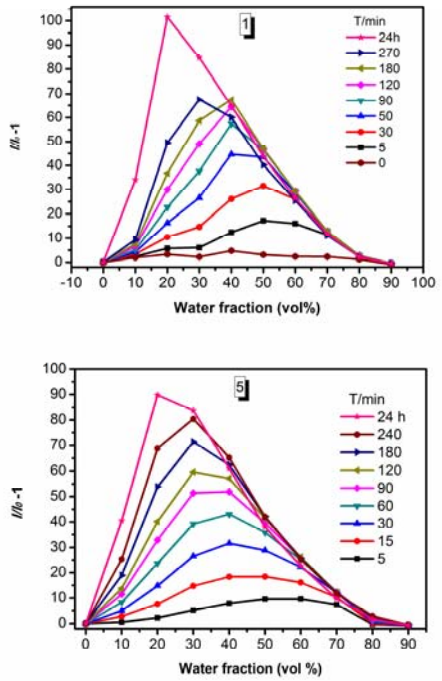

Fig. 6 Time-dependent of changes of **1** and **5** in the **PL** peak intensity (10 μM).

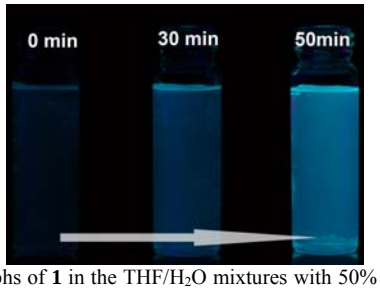

Fig. 7 Photographs of **1** in the THF/H_2O mixtures with 50% water contents at different times taken under UV illumination (10 μM).

SEM and TEM Observation

The scanning electron microscopy (SEM) images of **1**, **5** and **6** in the THF/water mixtures with low and high water contents at different time are shown in **Fig. 8**, which manifest the existence of aggregation in the solvent mixture. For **1** with 50% water content (**Fig. 8a**), the particle size was about 200-300 nm. Globular particle of **1** with 70% water content after water was injected for 1 hour (**Fig. 8b**) can be observed in a form of fusion. After water was injected for 2.5 hours, the molecules grew into larger rods in a round strips shape, with widths of ~200 nm and various length ranging from 200 nm-600 nm. Similar to **1**, **5** has a square structure after water was injected for 2 hours with 50% water content (**Fig. 8d**), indicating some kind of specific arrangement of molecules. **5** shows irregular round strips (**Fig. 8e**) after water was injected for 3 h with 70% water content, which is similar to **1** (**Fig. 8c**). Particles of **6** with 30% water content change from amorphous form (**Fig. 8f**) with diameter of nearly 150 nm after water was injected for 30 min to crystalline form (**Fig. 8g**) with diameter of 300-400 nm after water was injected for 3 h. Initially only a small portion of the compound molecules probably cluster together to form tiny nanoparticles. The larger portion of the compound molecules remaining in the solvent mixture then gradually deposits onto the initially formed nanoparticles in a way similar to recrystallization. The aggregations of **6** with 90% water content after water was injected for 30 min (**Fig. 8h**) can be observed in a form of globe. Almost no obvious change of diameters and morphology can be observed even after water was injected for 24 h in this solvent mixtures (**Fig. S6**).

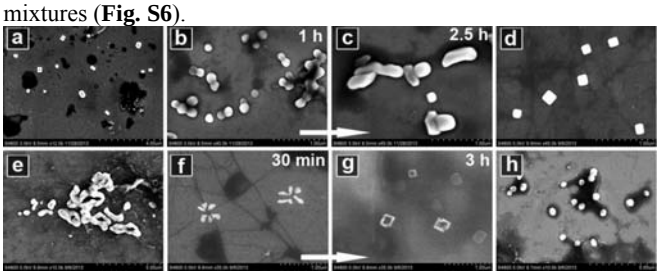

Fig. 8 SEM of **1** (a, 50%, 3 h , b ,70%, 1 h and c, 70% 2.5 h), **5** (d, 50% , 2 h and e, 70%, 3 h) and **6** (f, 30%, 30 min, g, 30%, 3 h and h, 90%, 30 min) formed in the THF/water mixtures containing different water contents in different time range after water was injected.

As shown in **Figure S7**, aggregates with an average diameter of ~670 nm formed in the aqueous mixture with 70% water content after water was injected for 30 min have grown up to ~1091 nm after water was injected for 3 hours. In comparison to the size of the aggregates of **6** at 70% water contents, no obvious change of diameters can be observed in spite of the interval of 23.5 hours, which is in accordance with the front speculation.

The transmission electron microscopy (TEM) images of **1** in the THF/water mixtures with different water contents (30%, 50%, 70% and 90%) are shown in **Fig. 9**. The insets of **Fig. 9 (a-d)** show the

electron diffraction (ED) patterns of the aggregates formed in the THF/water mixtures with 30%, 50%, 70% and 90% water contents, respectively. The dark regular structures in the photographs are the beam stop used to protect the detector from the intense main undiffracted beam. A series of clear diffraction spots surrounding the main undiffracted beam can be observed in **Fig. 9a**, indicating that the aggregates are crystalline or that the compound molecules are packed in an ordered fashion.[16] In the mixtures with low water fractions, molecules of **1** may cluster together slowly in an ordered fashion to form crystallike aggregations. When the water fractions becomes high (>80%), its molecules may aggregate instantly to form globular particles with no diffraction spots (**Fig. 9d**). As the water contents change from low to high, the quantity of diffraction spots verified from more to less. Since there are only dim diffraction ring observed in **Fig. 9d**, the nanoparticles are thus amorphous in nature.

The different rate of fluorescence intensity enhancement of compounds **1-6** in their solvent mixtures at the different water contents (**Fig. 6** and **Fig. S5)** may be attributed to the different speed of crystallization related to their different solvent environment.[17] As shown in **Fig. S8**, only two diffraction spots can be observed after water was injected for 40 min, however, many of them appeared (**Fig. S8b**) after 1 hour and 20 minute, which may account for the enhancement of fluorescence emission with time-dependent.

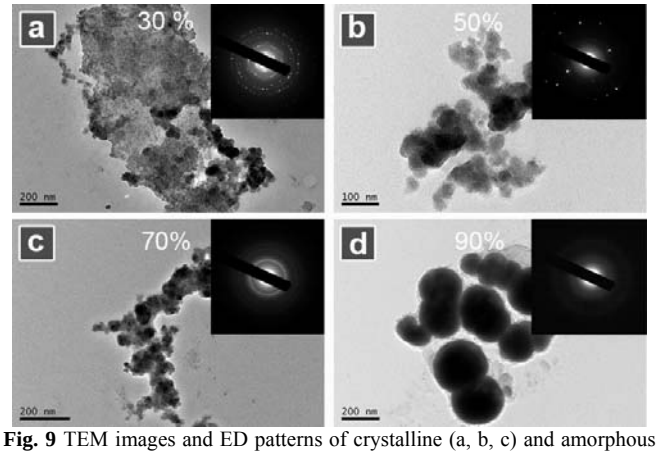

Fig. 9 TEM images and ED patterns of crystalline (a, b, c) and amorphous nanoaggregates of **1** formed in the THF/water mixtures containing 30% (a), 50% (b), 70% (c) and 90% (d) water contents after water was injected for 12 hours, 2 hours, 1 hour and 24 hours, respectively.

Different properties in different states

To gain further insight into the CEE properties of compounds **1-6**, we obtained a series of PL measurements in powder, film, the pure solution and mixed solutions with f_w = 30% (**Fig. 10** and **Fig. S9**). As we can see from **Table 2**, compounds **1** exhibit the value of λ_{em} as the order of the pure solution < the mixture solution (f_w = 30%) < film < powder. The same order can also be observed in **2**, **3**, **4**, **6**. (a) In the powder state, the molecules adopted the arrangement of relatively good planarity, which offer the molecules with relatively strong charge delocalization. (b) In the pure solution, the compounds are molecularly isolated without any interactions between the adjacent molecules. Hence, molecules may distort without the intermolecular restriction, giving an emission of blue-shift. (c) The molecules in the film state have emission wavelength similar to that in the state of powder, which is quite different from the wavelength in the pure solution. It is probably because the concentration of solution may increase as solvent evaporated gradually, majority of the isolated molecules agglomerated again.[18] (d) The curves of the mixture solution show a middle location by contrast to the other three states, which indicated that some weak force may be formed after water was injected to restrict the rotation of aromatic rings,[19] giving an red-shift emission by contrast to the location in the pure solution. As to the abnormal blue-shift of **5** in the state of powder, the reason may be that its molecules has a relatively larger aromatic rings, which enforce the molecules distort in a large extent to avoid complanation.[20]

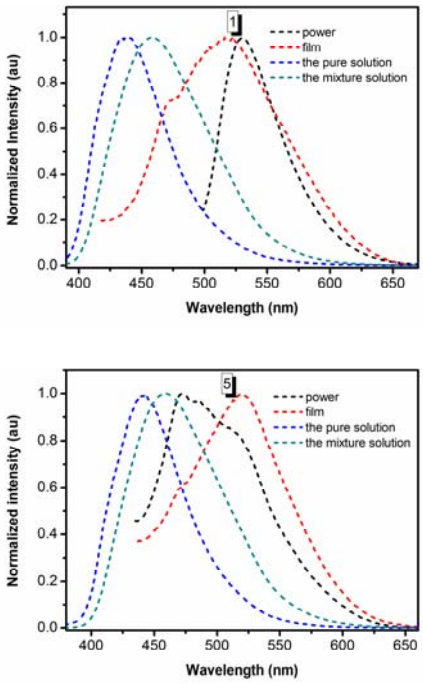

Fig. 10 Photoluminescence spectra of **1**, **5** in powder, film, pure THF solution and the solvent mixture with 30% water contents (10 μM) after the water was injected for 24 h.

Table 2 Maximum emission wavelength of **1-6** in different states.

	λ_{em}/nm					
	1	**2**	**3**	**4**	**5**	**6**
powder	531	-	537	523	472	548
film	516	-	531	513	520	544
THF	437	436	442	437	443	438
Mixtures	458	458	459	459	460	458
No signal of emission in powder and film can be obtained by **2**.						

Time-resolved fluorescence measurements of **1** and **5** were performed in **Fig. 11** (others in **Fig.S10**), and the detail data of the fluorescence decay curves of **1-6** are listed in **Table S3**. The experimental errors are estimated to be ±13% from sample concentrations and instruments. The lifetimes of **1-6** in different water fraction are obtained by monitoring at the monomer emission. The decay behavior of **1-6** is in a double-exponential manner in the mixture solution obtained by monitoring at the monomer emission. The lifetime of **1-6** in the water fraction of 0% is averagely contributed by the two lifetime species, while the lifetime of them in the water fraction of 30% and 60% is almost from the contribution of longer lifetime species. As shown in **Table 3**, the weighted mean lifetime of **1** in 30% water fraction (3.15 ns) is longer than that of **1** in 0% and 60% water fractions (2.14 ns and 1.73 ns, respectively). The same tendency can also be found in other five compounds, which implies that the formation of crystalline aggregates restricts the rotation and vibration of the groups in the molecules, so that longer emission lifetimes were

detected.[21] The relatively low water contents may make the molecules more conducive to self-organization. The lowest lifetimes was observed at 60% water content, which may be due to the combined action of the increasing solvent polarity and the amorphous aggregation.[22]

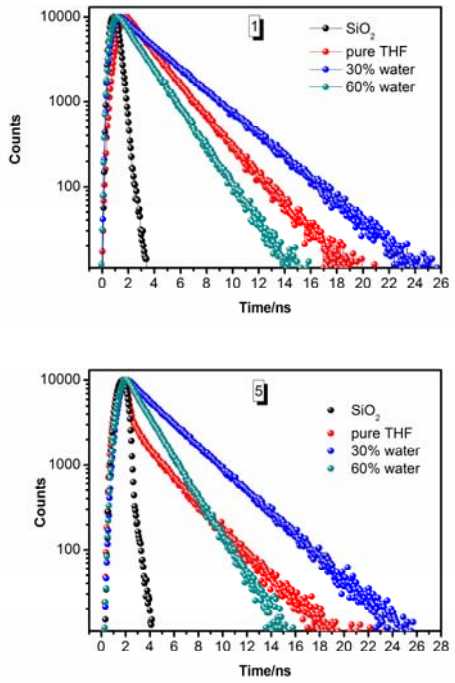

Fig. 11 PL lifetime spectra of **1**, **5** in pure solution, mixture solution with 30% water content and 60% water content (10 μM).

Conclusions

In summary, we have designed and synthesized six molecules (**1-6)** with different terminal aromatic ring. All the compounds are almost non-emissive when dissolved in pure THF, but become strong emissive when aggregated in aqueous solvents. Efficient emission enhancement can be achieved in relatively low water contents (≤ 60%) solutions contained crystalline phase, while low or even no emission are realized in the amorphous phase formed in solutions with high water contents (> 60%). When the water ratio reaches 20% (**1** and **5**) or 30% (**2**-**4**, **6**) after water was injected for 24 hours, the PL intensity reached the maximum. All compounds in mixture solvents with 30% and 60% water contents exhibits enhanced blue and cyan fluorescence emissions with time-dependent, respectively. The decreasing diffraction spots in aqueous mixtures with the increasing water contents suggests that compounds **1-6** are CEE-active materials. Evidently, a simple manipulation of the mixture composition or a small variation in the assembling environment may lead to the big change in the emission efficiency of **1-6**.

Experimental

General Information

All chemicals were available commercially. All the chemicals were used directly without further purification. THF was HPLC grade from BODI Organic Company and was used as received.

Instruments

The NMR spectra were recorded on a 400 MHz NMR instrument. Chemical shifts were reported in parts per million (ppm) relative to internal TMS (0 ppm) and coupling constants in hertz. Splitting patterns were described as singlet (s), doublet (d), triplet (t) or multiplet (m). IR spectra were recorded with a Nicolet FT-IR NEXUS 870 spectrometer (KBr discs). UV-*vis* absorption spectra were recorded on a UV-3100 spectrophotometer. The mass spectra were obtained on a autoflex speed MALDI-TOF/TOF mass spectrometer. The scan electron microscopy (SEM) and transmission electron microscopy (TEM) studies were performed using the Hitachi S-4800 scanning electron microscope and JEOL JEM-100SX transmission electron microscope. Dynamic light scattering (DLS) measurements were conducted on a Malvern Zeta Nano-ZS90 Particle Size Analyzer. Fluorescence measurements were carried out using an Edinburgh FLS920 fluorescence spectrometer equipped with a 450W Xe lamp and a time-correlated single-photon counting (TCSPC) card. For time-resolved fluorescence measurements, the fluorescence signals were collimated and focused onto the entrance slit of a monochromator with the output plane equipped with a photomultiplier tube. The absolute photoluminescence quantum yield (Φ_F) values of the mixture with different water fraction (0%, 30%, 60%, 90%; 1×10^{-5} M) were determined using an integrating sphere.

Preparation and characterization

Synthesis of a. Sodium hydroxide (24.0 g, 0.6 mol) and 4-iodo-phenol（120.0 g, 0.54 mol) were crashed together in batches with a pestle and mortar. And then bromoethane (300 mL) was added to this white powder. To this solution, cesium hydroxide (10 g) in 20 mL of DMF and 3 drops of 18-crow-6 was added and stirred for 1 h at room temperature. Then the reaction mixture was heated at 60 °C for 78 h. The mixture was concentrated and cooled to room temperature (RT) after the reaction was completed by monitoring with thin-layer chromatography (TLC). Much water was added to it and the mixture was extracted with dichloromethane(100 mL)three times. The organic extracts were dried over $MgSO_4$. After removing solvents under reduced pressure, red oily liquid was obtained (128.4 g, yield: 94.9%).

Synthesis of b. Aniline (5.0 g, 54 mmol) and 1-ethoxy-4-iodo-benzene (46.0 g, 185 mmol) were added to 1,2-dichlorobenzene (200 mL) in a three-neck flask. Potash (17.94 g, 130 mmol) and copper powder (8.34 g, 130 mmol) were slowly added to the mixture after stirred for a little moment in the atmosphere of nitrogen. Three drops of 18-crow-6 were added to the mixture. The mixture was reacted at 180 °C for 12 h. After the reaction was completed, it was cooled to RT. The solvents was removed under reduced pressure and the mixture was purified by chromatography on silica gel using petroleum ether/ethyl acetate (50:1, v/v) as eluent, give white crystals **b**, 7.8 g, yield: 43.6%. ^{1}H-NMR (400 MHz, $(CD_3)_2CO$), δ (ppm): 1.37 (t, J = 7.0 Hz, 6H), 4.04 (m, 4H), 6.86 (m, 7H), 7.02 (d, J = 8.4 Hz, 4H), 7.18 (t, J = 7.6 Hz, 2H).

Synthesis of c. $POCl_3$ (2.3 mL) was added dropwise to fresh distilled DMF (2.8 mL) which was stirred in flask (150 mL) using ice water bath cooling. After 30 min, the solution become sticky and stirred a little longer to yield a reddish salt resembling ice. Then the salt was combined with a portion of b (5.0 g, dissolved in 15 mL chloroform) to yield a reddish solution. Then the reaction mixture was heated at 65 °C for 10 h. The reaction was monitored by TLC. After the reaction was completed, it was concentrated. The black mixture was dissolved in dichloromethane and then poured into much water. Na_2CO_3 solution (40%) was added to adjust the pH of the mixture to 7-8. Then extract it three times with dichloromethane and the organic extracts were dried over $MgSO_4$. After removing solvents under reduced pressure, the mixture was

purified by chromatography on silica gel using petroleum ether/ethyl acetate (40:1, v/v) as eluent, giving yellow oily product 5.21g, yield: 96.15%. ^{1}H-NMR (400 MHz, $(CD_3)_2CO$), δ (ppm): 1.38 (t, J = 7.0 Hz, 6H), 4.07 (m, 4H), 6.78 (d, J = 8.8 Hz, 2H), 6.98 (d, J = 8.4 Hz, 4H), 7.19 (d, J = 8.8 Hz, 4H), 7.67 (d, J = 8.4 Hz, 2H), 9.759 (s, 1H).

Synthesis of d. A DMF solution containing 4-nitro-benzene-1,2-diamine (1.3 g, 8.3 mmol) and KI (0.55 g) was added to a DMF solution containing 4-[Bis-(4-ethoxyphenyl)-amino]-benzaldehyde (3 g, 8.3 mmol). The mixture was then refluxed by stirring for 16 h. After it was completed, the reaction mixture was cooled to room temperature and poured into water to yield large amount of precipitate. Then the precipitate was filtrated, washed with water three times. The crude product was purified by chromatography on silica gel using petroleum ether/ethyl acetate (5:1, v/v) as eluent, give red powdered solid 2.9 g, yield: 71 %. ^{1}H-NMR (400 MHz, DMSO-D_6), δ (ppm): 13.30 (s, 1H), 8.45-8.28 (d, J = 7.2 Hz, 1H), 8.11-8.06 (t, J = 8.6 Hz, 1H), 8.00-7.98 (m, 2H), 7.75-7.62 (m, 1H), 7.15-7.13 (d, J = 8.4 Hz, 4H), 6.97-6.95 (d, J = 8.8 Hz, 4H), 6.82-6.80 (d, J = 8.8 Hz, 2H), 4.05-4.00 (m, 4H), 1.35-1.32 (t, J = 6.8 Hz, 6H); MS (MALDI-TOF): m/z 493.575 [(M-1)$^+$, calcd 493.195].

Synthesis of e. Hydrazine hydrate (19 mL) was added dropwise to ethanol (50 mL) containing bis-(4-ethoxyphenyl)-[4-(5-nitro-1*H*-benzoimidazol-2-yl)-phenyl]-amine (1.9 g, 3.84 mmol). Then the mixture was refluxed by stirring for 20 min and 0.15 g $Pd(OAc)_2$ was added to the mixture. After stirring for one more hour, the solution was becoming to yellow transparent solution. The reaction mixture was then cooled to room temperature and concentrated. And yellow solid was obtained (1.456 g, 3.14 mmol), yield: 81.6 %. ^{1}H-NMR (400 MHz, DMSO-D_6), δ (ppm): 12.013 (s, 1H), 7.857-7.836 (d, J = 8.4 Hz, 2H), 6.487-6.468 (d, J = 7.6 Hz, 1H), 7.079-7.057 (d, J = 8.4Hz, 4H), 6.930-6.908 (d, J = 8.8 Hz, 4H), 6.781-6.083 (d, J = 8.8 Hz, 2H), 6.618 (s, 1H), 7.234-7.215 (d, J = 7.6 Hz, 1H), 4.874 (s, 2H), 4.029-3.977 (m, 4H), 1.341-1.307 (t, J = 6.8 Hz, 6H); MS (MALDI-TOF): m/z 463.936 [(M-1)$^+$, calcd 463.221].

Synthesis of Compounds 1-3. Compound 1: 0.3 g (0.43 mmol) 2-{4-[bis-(4-ethoxyphenyl)-amino]-phenyl}-1H-benzoimida zol-5-ylamine was added to a benzene solution (10 mL) and the mixture was stirred at 35 °C for a moment. Then a mixed solution of 0.046 g (0.43 mmol) Pyridine-2-carbaldehyde and two drops of glacial acetic acid was added to the mixture and the solid was dissolved quickly. The mixture was reacted for 15 h and then cooled to room temperature. Faint yellow powder was obtained through vacuum filtration (0.15 g), yield: 63.1 %. ^{1}H-NMR (400 MHz, DMSO-D_6), δ (ppm): 12.80 (s, 1H), 8.73 (s, 2H), 8.22-8.20 (d, J = 8.0 Hz, 1H), 8.01-7.99 (d, J = 8.4 Hz, 2H), 7.97-7.93 (t, J = 7.6 Hz, 1H), 7.65-7.63 (d, J = 8.4 Hz, 1H), 7.53-7.48 (m, 2H), 7.29-7.28 (d, J = 6.8 Hz, 1H), 7.11-7.09 (d, J = 8.4 Hz, 4H), 6.94-6.92 (d, J = 8.4 Hz, 4H), 6.84-6.82 (d, J = 8.4 Hz, 2H), 4.02-3.97 (m, 4H), 1.34-1.30 (t, J = 6.8 Hz, 6H); ^{13}C-NMR (100 MHz, DMSO-D_6), δ (ppm): 159.06, 156.25, 155.01, 153.36, 160.57, 150.18, 145.41, 139.64, 137.53, 128.17, 125.84, 121.53, 121.13, 118.06, 116.08, 63.75, 15.28; IR (KBr, cm^{-1}): 3379, 3150, 2976, 1611, 1546, 1506, 1472, 1447, 1393, 1284, 1241, 1194, 1167, 1115, 1048, 961, 923, 830; MS (MALDI-TOF): m/z 552.760 [(M-1)$^+$, calcd 552.248]. **Compound 2:** The synthesis of **2** is similar to that of **1**. Yield: 84.1 %. ^{1}H-NMR (400 MHz, DMSO-D_6), δ (ppm): 12.76 (s, 1H), 9.10 (s, 1H), 8.82 (s, 1H), 8.70-8.69 (d, J = 4.4 Hz, 1H), 8.35-8.33 (d, J =7.6 Hz, 1-H, d-H), 8.00-7.98 (d, J = 8.0 Hz, 2H), 7.62 (s, 1H), 7.56-7.43 (m, 2H), 7.25-7.24 (d, J = 6.8 Hz, 1H), 7.11-7.09 (d, J = 8.4 Hz, 4H), 6.94-6.92 (d, J = 8.4 Hz, 4H), 6.84-6.81 (d, J = 8.4 Hz, 2H), 4.02-3.97 (m, 4H), 1.34-1.31 (t, J = 6.8 Hz, 6H); ^{13}C-NMR (100 MHz, DMSO-D_6), δ (ppm): 156.93, 156.24, 153.15, 152.11, 150.87, 150.53, 146.14, 139.66, 135.29, 132.48, 128.14, 124.60, 121.19, 118.11, 116.09, 63.76, 15.28; IR (KBr, cm^{-1}): 3396, 3165, 2976, 1607, 1546, 1505, 1474, 1448, 1393, 1288, 1240, 1193, 1167, 1115, 1048, 962, 923, 828; MS (MALDI-TOF): m/z 552.248 [(M-1)$^+$, calcd 552.346]. **Compound 3:** The synthesis of **3** is aslo similar to that of **1**. Yield: 63.1 %. ^{1}H-NMR (400 MHz, DMSO-D_6), δ (ppm): 12.76 (s, 1H), 8.80 (s, 1H), 8.75-8.74 (s, J = 4.8 Hz, 2H), 7.98-7.96 (d, J = 8.4 Hz, 2H), 7.88-7.87 (d, J = 4.4 Hz, 2H), 7.63-7.62 (d, J = 6.8 Hz, 1H), 7.51-7.45 (m, 1H), 7.28-7.26 (d, J = 7.6 Hz, 1H), 7.13-7.11 (d, J = 8.4 Hz, 4H), 6.96-6.94 (d, J = 8.4 Hz, 4H), 6.83-6.80 (d, J = 8.4 Hz, 2H), 4.05-4.00 (m, 4H), 1.35-1.32 (t, J = 6.8 Hz, 6H); ^{13}C-NMR (100 MHz, DMSO-D_6), δ (ppm): 157.23, 156.25, 153.47, 150.95, 150.60, 145.44, 143.46, 139.63, 128.15, 122.64, 121.09, 118.09, 116.07, 63.75, 15.26; IR (KBr, cm^{-1}): 3414, 3145, 2977, 1602, 1550, 1504, 1476, 1448, 1394, 1286, 1239, 1192, 1167, 1115, 1045, 960, 922, 823; MS (MALDI-TOF): m/z 552.248 [(M-1)$^+$, calcd 552.030].

Synthesis of Compounds 4-6. Compound 4: 0.3 g (0.43 mmol) 2-{4-[bis-(4-ethoxyphenyl)-amino]-phenyl}-1H-benzoimidazol-5-ylamine was added to a methanol solution (10 mL) and the mixture was stirred at 35 °C for a moment. Then a mixed solution of 0.046 g (0.43 mmol) benzaldehyde and one drops of glacial acetic acid was added to the mixture and the solid was dissolved quickly. The reaction was monitored by TLC. Not until 9 hours after did the mixture completely reacted. Then the solvent was removed under vacuum. DMF (5 mL) was put into the product. The mixture was put into water (80 mL) after the product was fully dissolved. Yellowish white powder was obtained through vacuum filtration (0.32g), yield: 84 %. ^{1}H-NMR (400 MHz, DMSO-D_6), δ (ppm): 12.69(s, 1H), 8.72(s, 1H), 7.95-7.97 (d, J = 8.0 Hz, 4H), 7.61-7.35 (m, 5H), 7.21-7.17 (t, J = 8.2 Hz, 1H), 7.13-7.10 (d, J = 8.8 Hz, 4H), 6.96-6.94 (d, J = 8.8 Hz, 4H), 6.83-6.80 (d, J = 8.8 Hz, 2H), 4.05-4.00 (m, 4H), 1.35-1.32 (t, J = 6.8 Hz, 6H); ^{13}C-NMR (100 MHz, DMSO-D_6), δ (ppm): 158.66, 155.63, 152.38, 150.38, 149.88, 145.87, 139.09, 136.35, 134.24, 133.03, 131.65, 128.75, 128.45, 127.52, 122.71, 120.69, 119.24, 117.55, 115.5, 63.17, 14.68; IR (KBr, cm^{-1}): 3408, 2980, 1607, 1505, 1473, 1449, 1390, 1288, 1238, 1193, 1166, 1112, 1046, 962, 921, 830; MS (MALDI-TOF): m/z 553.396 [(M+1)$^+$, calcd 553.253]. **Compound 5:** 0.5 g (0.72 mmol) 2-{4-[bis-(4-ethoxyphenyl)-amino]- phenyl}-1H-benzoimidazol-5-ylamine was added to methanol solution (10 mL) and the mixture was stirred at 35 °C for a moment. Then a mixed solution of 0.112 g (0.72 mmol) 2-naphthaldehyde and one drops of glacial acetic acid was added to the mixture and the solid was dissolved quickly. The reaction was monitored through TLC. Not until 4 hours after did the mixture completely reacted. Yellowish white powder was obtained through vacuum filtration (0.55 g), yield: 84.8 %. ^{1}H-NMR (400 MHz, DMSO-D_6), δ (ppm): 12.722 (s, 1H), 8.889 (s,1H), 8.41 (s, 1H), 8.20-8.18 (d, J = 8.4 Hz, 1H), 8.05-7.97 (m, 5H), 7.61-7.43 (m, 4H), 7.27-7.25 (d, J = 8.0 Hz, 1H), 7.13-7.11 (d, J = 8.8 Hz, 4H), 6.96-6.94 (d, J = 8.8 Hz, 4H), 6.83-6.81 (d, J = 8.8 Hz, 2H), 4.04-4.01 (m, 4H), 1.35-1.32 (t, J = 6.8 Hz, 6H); ^{13}C-NMR (100 MHz, DMSO-D_6), 155.63, 152.43, 149.89, 139.09, 134.1, 132.74, 128.64, 128.40, 127.82, 127.53, 126.77, 123.58, 121.51, 120.68, 117.54, 115.51, 63.16, 14.68; IR (KBr, cm^{-1}): 2973, 1609, 1547, 1503, 1475, 1445, 1390, 1284, 1238, 1195, 1167, 1117, 1046, 962, 924, 827; MS (MALDI-TOF): m/z 603.417 [(M+1)$^+$, calcd 603.268]. **Compound 6:** the synthesis of compound **6** is almost the same as **5**. Yield: 98 %. ^{1}H-NMR (400 MHz, DMSO-D_6), δ (ppm): 13.50-13.43 (d, J = 27.6 Hz, 1H), 12.77-12.76 (d, J = 5.2 Hz, 1H), 9.04-9.03 (d, J = 3.2 Hz, 1H), 7.98-7.96 (d, J = 8.4 Hz, 2H), 7.70-7.63 (m, 2H), 7.52-7.49 (t, J = 7.2 Hz, 1H), 7.42-7.38 (t, J = 8 Hz, 1H), 7.31-7.28 (d, J = 8.4 Hz, 1H), 7.13-7.10 (d, J = 8.4 Hz, 4H), 7.00-6.94 (m, 6H), 6.83-6.81 (d, J =

8.8 Hz, 2H), 4.05-3.99 (m, 4H), 1.35-1.32 (t, J = 6.8 Hz, 6H); ^{13}C-NMR (100 MHz, DMSO-D_6): 160.2, 155.65, 152.82, 150.00, 144.71, 139.04, 134.44, 132.39, 130.72, 127.55, 122.26, 120.45, 119.45, 119.00, 117.49, 116.48, 115.51, 63.17, 14.67; IR (KBr, cm^{-1}): 2974, 1609, 1571, 1503, 1449, 1392, 1280, 1239, 1194, 1166, 1145, 1112, 1047, 963, 920, 827; MS (MALDI-TOF): m/z 569.416 [$(M+1)^+$, calcd 569.247].

Acknowledgment

This work was supported by the Program for New Century Excellent Talents in University (China), the Doctoral Program Foundation of the Ministry of Education of China (20113401110004), the National Natural Science Foundation of China (21271003, 21271004 and 51372003), the Natural Science Foundation of Education Committee of Anhui Province (KJ2012A024), the 211 Project of Anhui University, Higher Education Revitalization Plan Talent Project of (2013) and the Ministry of Education Funded Projects Focus on Returned Overseas Scholar.

Notes and References

[a]*College of Chemistry and Chemical Engineering, Anhui University and Key Laboratory of Functional Inorganic Materials Chemistry of Anhui Province, Hefei 230601, P. R. China.*
[b]*School of Materials and Chemical Engineering, Anhui Jianzhu University, Hefei 230601, P. R. China.*
[c]*Center of Modern Experimental Technology, Anhui University, Hefei 230039, P. R. China.*
[d]*School of Chemical Engineering, Hefei University of Technology, Hefei 230009, P. R. China.*
**Corresponding author. [a]Fax: +86-551-63861279, Tel: +86-551-63861279; [b]Fax: +86-551-63828106, Tel: +86-551-63828150.*

Electronic Supplementary Information (ESI) available: Fig.S1-S10, Tables S1-S3.

1 (a) K. T. Kamtekar, A. P. Monkman, M. R. Bryce, *Adv. Mater*., 2010, **22**, 572-582; (b) S. J. Park, S. G. Kuang, M. Fryd, J. G. Saven, S. J. Park, *J. Am. Chem. Soc*., 2010, **132**, 9931-9933.

2 (a) R. Jakubiak, C. J. Collison, W. Wan, L. J. Rothberg, B. R. Hsieh, *J. Phys. Chem. A*, 1999, **103**, 2394-2398; (b) S. W. Thomas, G. D. Joly, T. M. Swager, *Chem. Rev*., 2007, **107**, 1339-1386.

3 J. D. Luo, Z. L. Xie, J. W. Y. Lam, L. Cheng, H. Y. Chen, C. F. Qiu, H. S. Kwok, B. Z. Tang, *Chem. Commun*., 2001, 1740-1741.

4 (a) B. K. An, S. K. Kwon, S. D. Jung, S. Y. Park, *J. Am. Chem. Soc*., 2002, **124**, 14410-14415; (b) J. Chen, C. C. W. Law, J. W. Y. Lam, Y. Dong, S. M. F. Lo, I. D. Williams, D. B. Zhu, B. Z. Tang, *Chem. Mater*., 2003, **15**, 1535-1546; (d) J. Chen, H. Peng, C. C. W. Law, Y. Q. Dong, J. W. Y. Lam, I. D. Williams, B. Z. Tang, *Macromolecules*, 2003, **36**, 4319-4327.

5 (a) L. J. Qian, B. Tong, J. B. Shen, J. B. Shi, J. G. Zhi, B. Z. Tang, *J. Phys. Chem. B*, 2009, **113**, 9098-9103; (b) W. Z. Yuan, X, Y. Shen, H. Zhao, J. W. Y. Lam, L. Tang, B. Z. Tang, *J. Phys. Chem. C*, 2010, **114**, 6090-6099; (c) C. M. Yang, I. W. Lee, T. L. Chen, J. L. Hong, *J. Mater. Chem. C*, 2013, **1**, 2842-2850.

6 (a) J. W. Chen, B. Xu, B. Z. Tang, Y. Cao, *J. Phys. Chem. A*, 2004, **108**, 7522-7526; (b) K. Itami, Y. Ohashi, J. i. Yoshida, *J. Org. Chem.*, 2005, **70**, 2778-2792.

7 (a) W. Huang, H.T. Zhou, B. Li and J. H. Su, *RSC. Adv.*, 2013, **3**, 3038; (b) M. Liang, W. Xu, F. S. Cai, Z. M. Li, *J. Phys. Chem. C*, 2007, **111**, 4465-4472; (c) H. M. Tian, X. C. Yang, R. K. Chen, L. C. Sun, *J. Phys. Chem. C*, 2008, **112**, 11023-11033.

8 F. Sączewskia, P. J. Bednarski, R. Grünertb, *J. Inorg. Biochem*., 2006, **100**, 1389-1398.

9 L. K. Wang, Z. Zheng, Z. P. Yu, J. Zheng, J. Y. Wu, Y. P. Tian and H. P. Zhou, *J. Mater. Chem. C*, 2013, **1**, 6952-6959.

10 C. W. Chang, C. J. Bhongale, C. S. Lee, W. K. Huang, C. S. Hsu, E. W. G. Diau, *J. Phys. Chem. C*, 2012, **116**, 15146-15154.

11 W. Z. Yuan, Y. Y. Gong, S. M. Chen, X. Y. Shen, B. Z. Tang, *Chem. Mater.*, 2012, **24**, 1518-1528.

12 (a) Q. Q. Li, J. H. Zou, J. W. Chen, Z. J. Liu, Y. Cao, *J. Phys. Chem. B*, 2009, **113**, 5816-5822; (b) J. Liu, Q. Meng, X. T. Zhang, X. Q. Lu, P. He, W. P. Hu, *Chem. Commun*., 2013, **49**, 1199-1206.

13 (a) Y. Q. Dong, J. W. Y. Lam, A. J. Qin, Z. Li, B. Z. Tang, *Chem. Commun*., 2007, 3255-3257; (b) H. Tong, Y. Q. Dong, J. W. Y. Lam,, B. Z. Tang, *Chem. Commun*., 2006, 1133-1135.

14 T. Y. Han, Y. N. Hong, N. Xie, S. J. Chen, N. Zhao, E. G. Zhao, J. W. Y. Lam, H. M. H. Y. Sung, Y. P. Dong, B. Tong, B. Z. Tang, *J. Mater. Chem. C*, 2013, **1**, 7314-7320.

15 Y. Qian, S. Y. Li, G. Q. Zhang, Q. Wang, S. Q. Wang, H. J. Xu, G. Q. Yang, *J. Phys. Chem. B*, 2007, **111**, 5861-5868.

16 T. Tong, Y. N. Hong, Y. Q. Dong, B. Z. Tang, *J. Phys. Chem. B*, 2007, **111**, 2000-2007.

17 J. Wang, J. Mei, R. R. Hu, J. Z. Sun, A. J. Qin, B. Z. Tang, *J. Am. Chem. Soc*., 2012, **134**, 9956-9966.

18 Z. P. Yu, Y. Y. Duan, L. H. Cheng, Z. L. Han, H. P. Zhou, J. Y. Wu, Y. P. Tian, *J. Mater. Chem*., 2012, **22**, 16927-16932.

19 M. D. Yang, D. L. Xu, W. G. Xi, L. K. Wang, H. P. Zhou, J. Y. Wu, Y. P. Tian, *J. Org. Chem*., 2013, **78**, 10344-10359.

20 Z. Zheng, Z. P. Yu, M. D. Yang, F. Jin, Q. Zhang, H. P. Zhou, J. Y. Wu, Y. P. Tian, *J. Org. Chem*., 2013, **78**, 3222-3234.

21 C. Y. Bao, R. Lu, M. Jin, P. C. Xue, Y. Y. Zhao, *Org. Biomol. Chem*., 2005, **3**, 2508-2512.

22 X. Q. Zhang, Z. G. Chi, H. Y. Li, B. J. Xu, J. R. Xu, *J. Mater. Chem*., 2011, **21**, 1788-1796.

